Bulletin of Mathematical Biology (2006) 68: 223–2261
DOI 10.1007/s11538-006-9103-y

ORIGINAL ARTICLE

Modeling Intercellular Interactions in Early *Mycobacterium* Infection

Christina Warrender*[,a], Stephanie Forrest[a,b], Frederick Koster[c]

[a] *Department of Computer Science, University of New Mexico, P.O. Box 5800 MS 1423, Albuquerque, NM 87185-1423, USA*
[b] *Santa Fe Institute, 1399 Hyde Park Road, Santa Fe, NM 87501, USA*
[c] *Lovelace Respiratory Research Institute, 2425 Ridgecrest Drive SE, Albuquerque, NM 87108 5127, USA*

Received: 13 June 2005 / Accepted: 15 February 2006 / Published online: 20 May 2006

Abstract Infection with *Mycobacterium tuberculosis* (*Mtb*) is characterized by localized, roughly spherical lesions within which the pathogen interacts with host cells. Containment of the infection or progression of disease depends on the behavior of individual cells, which, in turn, depends on the local molecular environment and on contact with neighboring cells. Modeling can help us understand the nonlinear interactions that drive the overall dynamics in this system. Early events in infection are particularly important, as are spatial effects and inherently stochastic processes. We describe a model of early *Mycobacterium* infection using the CyCells simulator, which was designed to capture these effects. We relate CyCells simulations of the model to several experimental observations of individual components of the response to *Mtb*.

Keywords Tuberculosis · Stochastic simulation · Immunology

1. Introduction

Infectious agents enter the body through its most accessible tissues in the skin, lungs, and gut. The development of disease or immunity often depends on the initial interactions between the pathogen and immune system cells in these peripheral tissues. The spatial arrangement of local tissue cells, immune system cells, and pathogen may significantly affect the dynamics of these interactions. Highly organized local structures develop in some infections such as in tuberculosis. Stochastic effects, ranging from random encounters between individual cells to factors affecting gene expression within those cells, may also be important. Despite significant

*Corresponding author.
E-mail address: cewarr@sandia.gov (Christina Warrender).

progress in understanding the individual components of these localized responses, we still have a poor understanding of how those components interact to contain infection and the conditions under which this containment fails.

Modeling such systems can help us understand the nonlinear interactions that drive the overall dynamics. However, the complex spatiotemporal interactions involved are difficult to capture adequately in a mathematical model. Cell interactions are mediated by a large variety of molecular signals present on cell surfaces or secreted into the extracellular environment. Cell behavior therefore depends on exposure to neighboring cells, pathogens, and local concentrations of molecules, particularly cytokines. Complex dynamics within individual cells may affect how they respond to these external stimuli. It is therefore important that models capture the spatial relationships of cells with their neighbors, the molecular environment of the cells, and their internal state. This is best done with models that explicitly represent individual cells.

Multicellular models of this type are relatively new and becoming increasingly important. There are some specific models of tuberculosis (Segovia-Juarez et al., 2004) and other systems (see, for example, Dallon, 2000). However, there are few tools available to support development of multicellular models. We developed a multi-purpose simulator called CyCells that has the flexibility to accommodate models of many different kinds of multicellular systems. It uses a hybrid modeling approach; cells are represented explicitly, each with their own internal state, while extracellular molecular species are represented by their concentration. We previously used CyCells to model homeostasis of alveolar macrophages (Warrender et al., 2004); here, we describe a model of early *Mycobacterium* infection that illustrates CyCells' ability to capture spatial interactions between cells.

In order to allow modeling of many different kinds of cell behaviors, CyCells uses a computational abstraction known as Sense–Process–Act. Agent behaviors are segregated into three categories – those that handle sensing of the external environment, those that update the internal state, and those that implement concrete actions that affect the agent or its environment or both. Simulation models are defined by describing the sense, process, and act functions appropriate for each cell type in the model. Sensing includes both sensing the local molecular concentration and sensing neighboring cells. Processing functions correspond to intracellular signaling in real cells. However, for the purpose of modeling multicellular dynamics, capturing the basic input–output behavior of the cells is sufficient, so we abstract away many of the details of intracellular signaling pathways. Cell actions – death, division, differentiation, movement, etc. – may occur constitutively or be triggered by changes in cell state. A few specialized functions of each type serve to cover a wide range of cell behaviors.

The choice of which cell behaviors and other components to include in a model represents a hypothesis about which elements of the modeled system are most important. The resulting model is necessarily a simplification of the real system, but it can nevertheless be used to explore the relative contributions of these key components. We illustrate this approach with our model of the early stages of infection with *Mycobacterium tuberculosis* (*Mtb*), the pathogen that causes tuberculosis. Our model includes cytokines shown to be key players in *Mtb* infection that have been studied in experimental systems. We relate CyCells simulations of this

model to a wide variety of experimental observations of individual components of the response to *Mtb*.

2. Tuberculosis

Approximately one-third of the world population is infected with *Mtb* but only 10–20% develop clinical disease, usually after a latent period of many years (Corbett et al., 2003; Stewart et al., 2003). Inhaled bacteria that reach the lower airways are phagocytosed (ingested) by macrophages. In non-immune hosts *Mtb* adapts to survive intracellularly and replicate. When the infected cells die, the bacilli spread to uninfected macrophages recruited during the inflammatory response initiated by the original infected cells (Dannenberg and Rook, 1994).

Experiments in mice and other animals show a common trend after aerosol infection with *Mtb*; bacteria replicate in the lungs for approximately 3 weeks, then the bacterial load stabilizes (North and Jung, 2004). Duration of the growth phase and peak bacterial load may vary with the inbred mouse strain, the *Mtb* strain, and initial dose size; Rhoades et al. (1997) show bacterial loads of 100–2000 times the initial dose approximately 3 weeks after infection. Stabilization of the bacterial load is thought to coincide with the expression of T cell immunity in the lungs (North and Jung, 2004). T cells are also thought to be important in control of human tuberculosis because depletion of T cells is associated with accelerated disease (Kaufmann, 2001). However, the exact mechanisms and dynamics of pathogen control are not completely understood.

Bacterial control is thought to depend on the formation and maintenance of *granulomas* in the lungs. These are roughly spherical lesions in which bacilli are contained by immune system cells. Although there may be multiple infected sites, lesions develop independently of each other (Dannenberg and Rook, 1994). Granulomas are complex structures that develop over time, but they begin as localized aggregations of macrophages in which bacteria replicate. This initial growth is thought to be slowed or halted by T cell activation of macrophages. In response, *Mtb* may use multiple evasion strategies to persist in a state that is less detectable by the immune system (Wayne and Sohaskey, 2001; Shi et al., 2003). Although the total bacterial load is fairly stable after this point, lesions in mice show continued pathological progression (Rhoades et al., 1997).

2.1. T cells and macrophage activation

Under appropriate conditions, macrophages are activated to increase their ability to kill recently ingested pathogens. However, chronically infected macrophages lose their ability to become activated (Janeway et al., 1999). Without continued stimulation, activated macrophages may become deactivated. In vitro, murine macrophages can be activated to kill *Mtb* by adding the appropriate cytokines, but human macrophages seem also to require the presence of T cells (Bonecini-Almeida et al., 1998). Brookes et al. (2003) suggest that contact between T cells and macrophages is required for full macrophage activation. Some contact is

certainly required in vivo because recruited T cells do not produce cytokines until they recognize antigen presented by macrophages in the infected tissue (Janeway et al., 1999).

Before T cells are recruited to the lungs, they must be sensitized in the lymphoid organs to initiate expansion of the *Mtb*-specific T cell pool (Jenkins et al., 2001). In mice, *Mtb*-specific T cells are first detected in the lungs about 2 weeks after infection (Chackerian et al., 2002). The recruited T cells recognize a wide variety of antigens, including some that may not be specific to *Mtb*. Such heterogeneity is characteristic of many immune responses but is not required for effective granuloma formation (Hogan et al., 2001). As there is insufficient data to quantitate the contributions of different T cell subpopulations, we include only a single T cell population in our model.

2.2. Cytokines in tuberculosis infection

Macrophages and T cells produce many cytokines that promote or inhibit macrophage activation. A few of the cytokines thought to be most important in control of intracellular infections in general and tuberculosis in particular are tumor necrosis factor-α (TNF), interleukin-10 (IL-10), and interferon-γ (IFN-γ). Protective roles for IFN-γ and TNF have been demonstrated in *Mtb* infection; the role of IL-10, which downregulates many immune system functions, is more controversial (Kaufmann, 1999). IFN-γ is produced primarily by T cells and NK cells and appears to be the most important cytokine for macrophage activation (Ma et al., 2003).

Phagocytosis of many pathogens, including *Mtb*, induces macrophages to produce TNF (Kaufmann, 1999). Macrophage production of TNF begins soon after infection but is transient (Thomson, 1994). T cells may also be induced to produce TNF; the amount of TNF produced by T cells is generally much greater than that from macrophages (Barnes et al., 1993; Engele et al., 2002). TNF is a pleiotropic cytokine; it has been observed to have many different effects on a variety of cell types, some of which are contradictory and many of which are not completely understood. One of the better-known effects, however, is to induce production of chemokines and expression of adhesion molecules on endothelial cells to facilitate migration of immune system cells from circulation into infected tissues (Thomson, 1994). TNF also synergizes with IFN-γ to activate macrophages, although it is apparently incapable of activating macrophages alone (Ding et al., 1988; Flesch and Kaufmann, 1990).

IL-10 is an anti-inflammatory cytokine produced by both macrophages and T cells in response to inflammatory signals. It inhibits macrophage activation and production of cytokines. IL-10 is thought to be important in keeping immune responses in check, but it may also permit pathogen growth when responses are damped excessively (Moore et al., 2001).

3. CyCells

To help understand localized immune responses such as the early response to *Mtb*, we need modeling approaches that can relate population-level dynamics

to individual cell interactions and responses to cytokines. CyCells is a three-dimensional, discrete-time simulator for studying intercellular interactions like those described in the previous section. Many features are designed for modeling intracellular infections. The code is written in C++, has been tested under Linux, and is available under the GNU General Public License. The basic simulation algorithm was published without a description of the spatial representation (Warrender et al., 2004). We briefly describe CyCells here, emphasizing the spatial components of the system. More detail is given in the user manual, which can be found with the code at https://sourceforge.net/projects/cycells/.

CyCells is a hybrid simulator in which models can include discrete and continuous components, and deterministic and stochastic dynamics. Individual cells are represented explicitly, but molecules are represented by their concentration. It is convenient to represent large numbers of nearly identical molecules by their overall concentration. However, the numbers of cells involved in the earliest stages of infection are relatively small, making continuous representations inappropriate for cell populations. There is also a great deal more variation between cells than between molecules. Even when larger cell populations are involved, modeling individual cells can help clarify the effects of cellular heterogeneity and differing spatial environments. CyCells models can also mix discrete and continuous representations within each cell. Because the extracellular molecular environment is represented continuously, it is often easiest to describe a cell's perception of that environment as a continuous value. However, for convenience, we discretize cell states. An example is macrophage activation, discussed in Section 2.1. Macrophages demonstrate a wide range in production rates of various antimicrobial molecules and cytokines associated with activation, so that each macrophage can differ in the degree to which each function is expressed, but we refer to cells as either activated or not activated. Other complex changes in cell state, for example, during death, division, and differentiation, are similarly treated as discrete events.

Individual components of internal cell state, whether continuous or discrete, can change deterministically or stochastically. Sensing of the extracellular molecular environment is governed by deterministic receptor kinetics; changing activation status is stochastic. Some of the heterogeneity between cells of the same type is due to inherently stochastic processes, which can be represented in individual-based models by stochastic interaction rules. At the start of an immune response, when small numbers of cells are involved, random events may have a significant effect on the eventual outcome. Incorporating stochastic dynamics also allows models to explore a distribution of system behaviors rather than just the average behavior that would be described by a deterministic model.

Our simulator implements a general framework for modeling multicellular systems. Different systems can be simulated by using different model definitions. The general process of model definition was explained in our earlier paper (Warrender et al., 2004). Here, we focus on the representation of space in CyCells and how it affects cell behavior. CyCells is designed to simulate spatially explicit models (although it is also possible to ignore spatial effects, as was done in Warrender et al. (2004)).

3.1. The tissue compartment

Cell behavior depends on local concentrations of cytokines and on interactions with neighboring cells. In CyCells, a volume of tissue is represented as a cubical compartment containing molecules and cells. This compartment can be subdivided into cubical patches to represent the spatial variance of molecular concentrations. Cells have explicit positions within the compartment. Molecular concentrations and cell positions change over time through molecular diffusion and cell movement. Periodic boundary conditions are used for changes in both molecular concentrations and cell positions to avoid edge effects. In other words, the simulated space "wraps around"; opposing boundaries are topologically connected so that cells or molecules that would exit one boundary re-enter from the opposite side.

The simulated volume is divided into regular cubes, or three-dimensional patches, where the patch size (set at run time) determines the spatial resolution of molecular concentrations. Molecular diffusion is implemented on this grid, as explained in the appendix. Concentrations decay uniformly at a fixed rate, or change through the actions of cells in specific patches.

3.1.1. Cell positions

A tissue-level model may include multiple cell types of varying sizes in nonuniform spatial distributions. Inflammation, in particular, may cause localized regions of high densities. A lattice scheme for cell positions does not adequately capture these spatial irregularities. In CyCells, cell positions are represented by continuous-valued coordinates to allow greater flexibility in spatial distributions. These coordinates specify the position of the center of a cell, which is represented as a sphere for simplicity. Cells adjust their positions to balance pressure from other cells and their own motive forces (explained in Section 3.1.3). To account for the fact that real cells can change shape to pack tightly, the spheres representing simulated cells may overlap when cell densities are high. However, the repulsive force between cells increases with increasing overlap.

3.1.2. Cell influx

In our model of the peripheral immune response in the lung, new cells arrive from the circulation, but blood vessels are not explicitly simulated. Some models assume that new cells enter only at the boundaries of the simulated compartment. Since any reasonably sized tissue has numerous blood vessels running through it that allow circulatory cells easy access to all parts of the tissue, CyCells allows addition of new cells anywhere in the simulated volume. Although the exact layout of the vasculature is not of interest here, the possibility of influx rates varying in different parts of the tissue due to local expression of cytokines and chemokines is important.

In CyCells, influx of new cells is controlled by cells already in the simulated tissue. One of the actions that can be defined for a cell type is the ability to admit new cells into the simulation. This allows cells to mimic the action of endothelial or epithelial cells in controlling cell migration. The probability with which a simulated endothelial cell admits a new cell may depend on the local cytokine environment.

For example, if a simulation has endothelial cells distributed throughout the tissue but the concentration of an inflammatory cytokine is high only in a small region, the rate of new cell entry will be increased there.

3.1.3. Cell movement

Cell movement in isotropic environments can be modeled as a persistent random walk (Lauffenburger and Linderman, 1993). Cells move at a nearly constant velocity over a short period of time, then change direction. The average time between direction changes is known as the persistence time. In the presence of chemokines, cell orientation is no longer random, but the general movement pattern is similar.

CyCells' movement actions govern how and when simulated cells choose their orientation. A simulated cell may move randomly or by chemotaxis. In chemotactic movement, the cell's orientation is chosen to match the direction of a local molecular gradient. If there is no detectable gradient, the cell chooses a direction at random. Unimpeded cell speed is assumed to be constant in these simulations, and it is the same for all cells of the same type. A cell's current orientation and the speed for its type determine its velocity vector in the absence of collisions.

Collisions in CyCells are inelastic. Simulated cells are represented as spheres for convenience, but those spheres are allowed to overlap to account for the fact that real cells are deformable. There is an ad hoc repulsive force when cells overlap that tends to move them apart, space permitting, and that prevents cells from moving directly through each other. This is implemented by adding a velocity component from an overlapping neighbor to a moving cell's unimpeded velocity vector. The magnitude increases linearly with the amount of overlap; the direction is from the neighbor cell center to the moving cell center. On each time step, the net velocity for each moving cell is calculated by summing its unimpeded velocity and the contributions from any overlapping neighbors, and is multiplied by the time step to get the cell's displacement. Final positions are corrected to account for periodic boundary conditions if necessary.

3.2. Individual cell behavior

This section describes aspects of internal cell state that were not addressed in Warrender et al. (2004). Some of these are due to the explicit representation of the spatial environment, while others are due to the interactions of macrophages with bacteria.

3.2.1. Sensitivity to the local environment

Cells can sense extracellular molecules or other cells. In simulation, the key point is to make appropriate changes to a cell's internal state in response to the local molecular environment or contact with neighboring cells. These changes may be described deterministically, especially in the case of continuously valued variables. Cell perception of the local molecular environment is often modeled deterministically. However, discrete changes in cell state may be triggered either by a continuous variable passing a threshold or by a stochastic event.

A cell's position is used to determine which three-dimensional patch represents the local molecular environment for that cell. A cell is sensitive to molecular concentrations only in the patch that it occupies. Similarly, any changes made to the concentration by the cell are applied only to the same patch.

Cell position determines which cells can interact. Cells are made sensitive to other cells by adding a sensing function to their model definitions. This function specifies the type of cell that can be detected and a distance limit on detection. The distance limit can exceed the sensing cell's radius because cells can extend pseudopods to increase their detection range.

3.2.2. Phagocytosis

In order for a macrophage to ingest a target cell, such as a bacterium, the cells must bind. The distance between cells and the number of target-specific receptors on the macrophage's surface both affect binding probability. There is a large variety of receptor types that mediate phagocytosis in real cells, and they vary in affinity for pathogen surface molecules and efficiency of inducing phagocytosis (Aderem, 2003). Macrophages vary in their levels of receptor expression and therefore in their ability to phagocytose pathogens.

In CyCells, this heterogeneity is represented by giving each simulated macrophage an attribute representing its phagocytic capability for a particular target type, expressed as a random value between 0 and 1. A cell with phagocytic capability greater than a threshold value ϕ will phagocytose a target cell within distance h. The target cell is removed from the extracellular environment and the macrophage's internal state is updated to reflect the number of targets ingested.

The fraction of the cell population that can phagocytose a given target is $1 - \phi$; if $\phi = 0$, all cells can phagocytose that target. Increasing values of ϕ represent increasing difficulty of phagocytosing the target or decreasing phagocytic competence of the macrophage population.

3.2.3. Intracellular infection

Macrophages destroy many things that they phagocytose, but some pathogens such as *Mtb* are able to establish an infection inside macrophages. Pathogens that have infected a cell are not represented as encapsulated objects but rather as one variable of the host cell's internal state. This variable represents the number of intracellular pathogens, which is a small integer value. If the host cell dies in a way that can release these pathogens, this number is used to create the appropriate number of new pathogen cells. (Unlike intracellular bacteria, extracellular bacteria are represented as distinct objects.)

The number of intracellular pathogens can change due to division or death of pathogens within the cell. The rate at which pathogens divide or die intracellularly depends on genetic factors (not modeled here) of both the bacteria and the host cells, and the degree to which the host cell has been activated to kill intracellular bacteria. We assume an intracellular division rate g and a death rate q that may vary over time but are constant during any given time step Δt. For the time step size and rates used in our simulations, there is likely no more than one birth or death event in a given time step. Therefore, the simulator increments

the intracellular population m by 1 with probability $gm\Delta t$ or decrements it with probability $qm\Delta t$.

4. TB model

We model the development of a single nascent granuloma in a small volume of tissue. Our model does not attempt a structurally correct representation of the lung and its airspaces, but we use data on recruitment to the lung in response to *Mtb* to refine the model. The most important characteristics to capture in this first model are the interactions between key cell and cytokine types; more anatomic detail could be incorporated later.

The TB model components are the three cytokines TNF, IL-10, and IFN-γ; uninfected, newly infected, and chronically infected macrophages; and T cells. The three cytokines represent the influence of many types of cytokines involved in the real system; in particular, TNF in the model is a surrogate for an array of chemokines as well as TNF itself. We also simulate endothelial cells that represent entry points for recruited cells but not cytokines produced by these cells.

Changes in cell state representing infection, activation, and changes in cytokine production are illustrated schematically in Fig. 1. Detailed descriptions of the transitions shown in Fig. 1 are given in the appendix; the parameters are summarized in Table 1. Briefly, macrophages become infected by phagocytosing *Mtb*. Infected macrophages may become capable of producing cytokines and/or killing intracellular *Mtb*, depending on the local cytokine environment. Both macrophages and T cells contribute to this cytokine environment. Eventually, infected macrophages lose the ability to acquire these functions and become chronically infected.

Our model of cytokine production and regulatory effects is based largely on in vitro studies of cell cultures. These include some rather complicated feedback interactions, but the model is still vastly simpler than the real system. In general, the effect of these feedback loops is to regulate cell recruitment and macrophage activation. This includes indirect effects, as some of the cytokines regulate cytokine production. The simulations are used to determine how well these feedback interactions, operating between individual neighboring cells, can capture key aspects of the infection dynamics in tissue. Most model parameters were chosen to try to match data from human cells, partly because most culture studies of alveolar macrophage responses to *Mtb* use human cells. However, early infection dynamics in humans are not observable, so simulation results are compared to observations in mice.

The simulations represent the developing infection in a $1\,\mathrm{mm}^3$ volume. One thousand simulated endothelial cells are randomly distributed throughout this volume, allowing influx rates to vary according to local cytokine concentrations. Each simulation represents the development of a single nascent granuloma, and is therefore initialized with a single *Mtb*-infected macrophage in the center of the volume. One thousand uninfected macrophages are also present initially, but no T cells. We used a time step of 20 s and a molecular grid size of $50\,\mu$m.

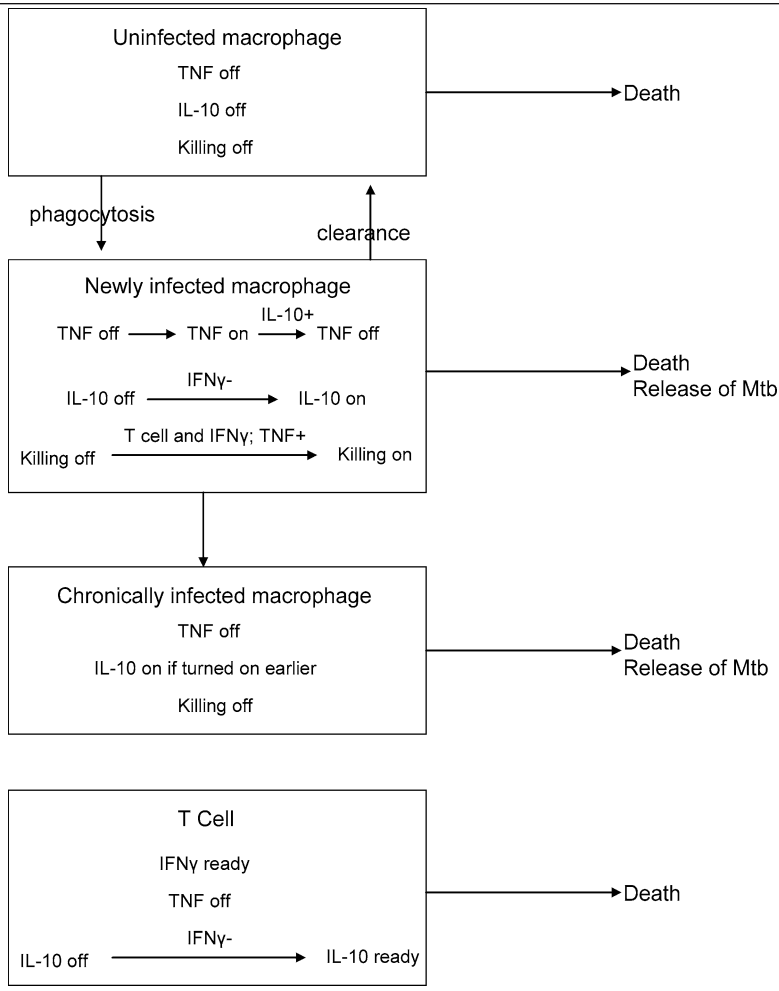

Fig. 1 Schematic of TB model showing macrophage and T cell behaviors. Labels inside the boxes represent cell states, *arrows* represent transitions between states, and labels on the *arrows* represent enabling conditions for transitions to take place. Most cytokine production is inducible rather than constitutive; this is indicated by the transitions from "off" to "on" or "ready." T cell secretion is marked as "ready" rather than on because T cells only secrete these cytokines when in contact with a newly infected macrophage. Only newly infected macrophages can become activated; this is indicated by the transition between (bacterial) "killing off" and "killing on." T cell contact and detectable IFN-γ are required for macrophage activation. IL-10+ indicates that presence of IL-10 increases the transition probability; IFN-$\gamma-$ indicates a negative effect of IFN-γ on the transition probability.

5. Simulation results

As mentioned in Section 4, our model simplifies the regulatory feedback loops present in real tissues. The simulations were designed to test how well the model captures dynamics observed in tuberculosis infection despite the simplifications. In the following first two sections, we explore system dynamics with the base

Table 1 Base parameters for TB model.

Parameter	Meaning	Value	Source
ϕ	Phagocytic threshold	0.7	Engele et al. (2002)
g	Intracellular *Mtb* growth rate	0.5 per day	Silver et al. (1998), MacMicking et al. (2003)
$q_{\max}$	Maximum intracellular *Mtb* kill rate	Varied	Bonecini-Almeida et al. (1998)
N	Maximum no. of bacilli/macrophage	50	Wigginton and Kirschner (2001)
$a_{\max}$	Maximum macrophage activation rate	1 per day	Schroder et al. (2004)
a_{TNF}	Effect of TNF on activation rate	1/100 pM	Estimate
$u_{\max}$	Maximum rate of chronic infection	0.1 per day	Estimate
v_{on}	Infected cell TNF "turn on" rate	1 per day	Engele et al. (2002)
v_{off}	Maximum infected cell TNF "turn off" rate	1 per day	Engele et al. (2002)
$w_{\max}$	Maximum IL-10 "turn on" rate	2 per day	Engele et al. (2002)
$m_{\mathrm{IL-10}}$	Half-sat constant, IL-10	25 pM	Wigginton and Kirschner (2001)
m_{IFN}	Half-sat constant, IFN-γ	100 pM	Estimate
p_{MTNF}	Macrophage TNF secretion rate	600 molecules/cell/s	Engele et al. (2002)
$p_{\mathrm{MIL-10}}$	Macrophage IL-10 secretion rate	60 molecules/(cell s)	Fulton et al. (1998), Engele et al. (2002)
p_{TIFN}	T cell IFN-γ secretion rate	200 molecules/(cell s)	Barnes et al. (1993), Tsukaguchi et al. (1999)
p_{TTNF}	T cell TNF secretion rate	2000 molecules/(cell s)	Barnes et al. (1993), Tsukaguchi et al. (1999)
$p_{\mathrm{TIL-10}}$	T cell IL-10 secretion rate	1 molecule/(cell s)	Barnes et al. (1993), Tsukaguchi et al. (1999)
i	Homeostatic influx rate	1.4 cells/(ml s)	Blusse van Oud Alblas et al. (1983)
$i_{\max}$	Maximum recruitment rate	100 cells/(ml s)	Serbina and Flynn (1999)
i_{half}	Half-saturation, TNF on influx rate	10 pM	Estimate
l_{M}	Macrophage death rate	0.12 per day	Chosen to balance i
l_{T}	T cell death rate	0.23 per day	Reinhardt et al. (2001)
h_{T}	Macrophage–T cell contact distance	10 μm	Estimate
b	Cytokine decay rate	0.07/min	Fishman and Perelson (1999)
D	Cytokine diffusion rate	10^{-8} cm^2/s	Young et al. (1980)

Note. Unless otherwise noted, $i_{\max}$ and i_{half} apply to both macrophages and T cells, but i affects only macrophage influx. Note that many of these parameter values are not explicitly given in the cited references, but estimates are based on data available in those references.

parameter values chosen from in vitro studies. The remaining sections study perturbations to the model corresponding to experimental model systems.

5.1. Outcome variability with base parameter set

There is considerable variation in simulation results for a single parameter set (Table 1) due to the stochastic properties of the model. This is illustrated for *Mtb* and macrophage counts in Fig. 2. *Mtb* were eliminated in 1 of the 30 simulations for this parameter set. However, bacterial growth in some simulations was very high, with a range over 3 logs growth in 3 weeks. There is similar variability in nature; lesions with different characteristics have been observed in different locations within the same animal (Rhoades et al., 1997; Davis et al., 2002).

The total bacterial burden in mouse lungs is the net result of growth within many independent lesions. In order to compare simulation results to those from

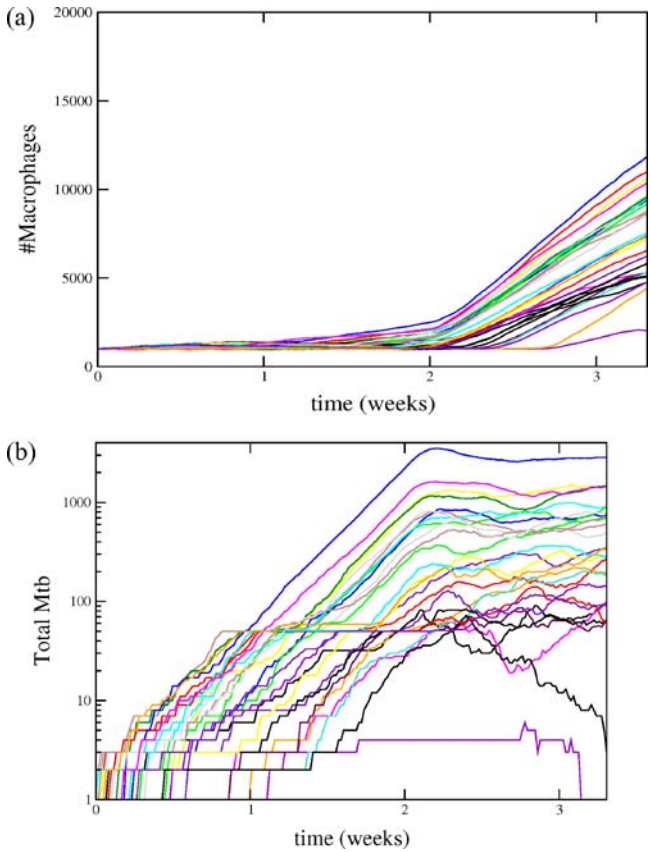

Fig. 2 Outcome variability for TB model with base parameter set. Total numbers of macrophages (*a*) and *Mtb* (*b*) over time for 30 simulations of the base parameter set. $q_{\max} = 2$ per day; other parameter values are same as shown in Table 1. T cell influx began 2 weeks after the start of infection.

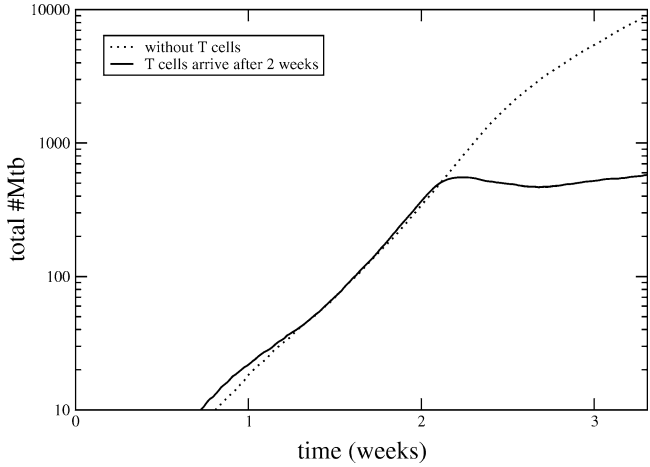

Fig. 3 Average simulated *Mtb* growth with base parameter set. $q_{\max} = 2$ per day; other parameter values are same as shown in Table 1.

experiments, we use the average simulated *Mtb* growth. This is shown in Fig. 3 for the simulations plotted in Fig. 2. For comparison, Fig. 3 also shows results from a set of simulations in which there were no T cells. The general trend matches that seen in experiments (North and Jung, 2004) where initial exponential growth is arrested shortly after the arrival of T cells. Cytokine concentrations are also within physiologic ranges (not shown).

5.2. Lesion structure

Spatial distributions of cells have a significant effect on infection outcome. Figure 4 shows a graphical illustration of the 3-week lesion from the worst-case simulation in Fig. 2 (the topmost line in the second panel). The figure shows an aggregation of uninfected and infected macrophages and T cells. T cells tend to cluster, presumably in areas of high TNF concentration. These clusters include many newly infected cells, which can produce TNF and induce T cell production of TNF. Macrophages within these clusters can become activated to kill *Mtb*. However, T cells may also linger in areas where infected cells have died or cleared their pathogens but the TNF concentration is still high. T cells not in contact with a newly infected macrophage do not produce cytokines. Infected cells on the fringes of these clusters may receive inadequate T cell and cytokine stimulation, particularly once they stop secreting TNF. These are the cells most likely to become chronically infected and allow continued bacterial growth.

There are no extracellular *Mtb* in Fig. 4, and the infection is contained. In contrast, simulations without T cells produced lesions like that shown in Fig. 5, containing larger numbers of infected cells and significant numbers of extracellular *Mtb*. (Despite the spread of infection, there are still large numbers of uninfected cells because a large percentage of the macrophages are unable to phagocytose *Mtb*.)

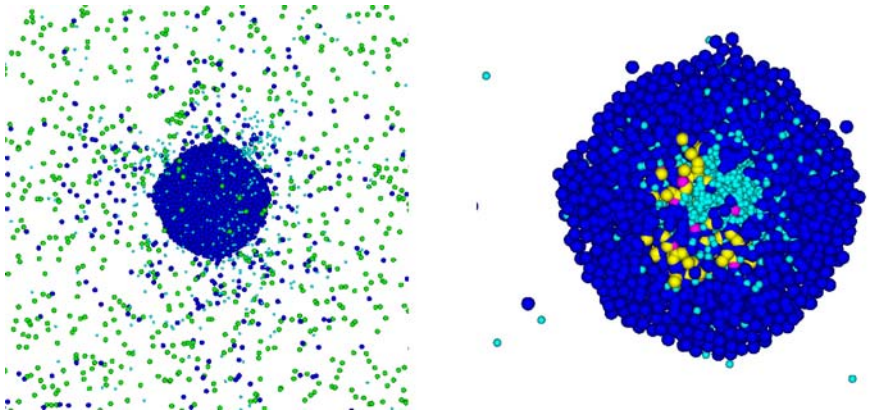

Fig. 4 Simulated lesion with base parameter set. *Left panel*: screenshot of the entire simulated volume. *Right panel*: thin slice through the center of the lesion. The green tissue cells were removed from the figure on the right to make it easier to distinguish the remaining cell types. Large dark blue cells are uninfected macrophages, large yellow cells are newly infected macrophages, large magenta cells are chronically infected macrophages, and smaller cyan cells are T cells. There are no extracellular *Mtb* in this image. $q_{\max} = 2$ per day; other parameter values are same as shown in Table 1.

Figure 4 shows a tight cluster of T cells in the center of the simulated lesion. Rhoades et al. (1997) describe T cells and B cells in early lesions as being clustered around blood vessels or around activated macrophages, but apparently this does not result in a large clump of T cells like that seen in Fig. 4. The tight cluster in the simulation is due in part to the lack of real tissue structure, which

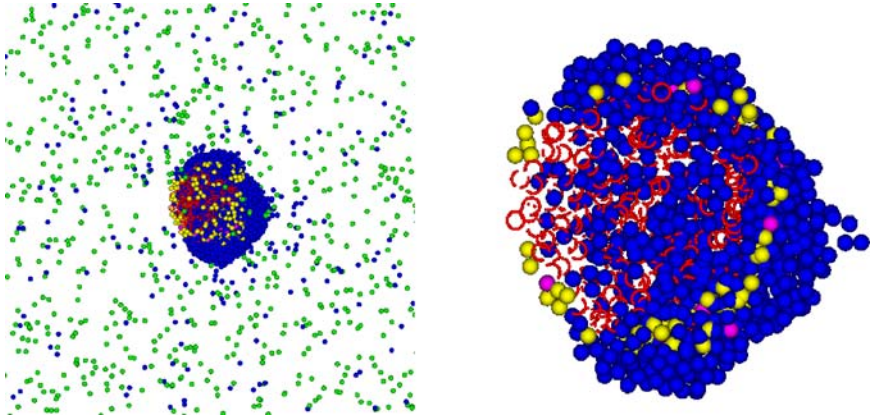

Fig. 5 Simulated lesion without T cells. *Left panel*: screenshot of the entire simulated volume. *Right panel*: thin slice through the center of the lesion. The green tissue cells were removed from the figure on the right to make it easier to distinguish the remaining cell types. Large dark blue cells are uninfected macrophages, large yellow cells are newly infected macrophages, large magenta cells are chronically infected macrophages, and the very small red cells and arcs are extracellular *Mtb*. Parameter values shown in Table 1.

allows cells to pack densely and also allows the lesion to grow around simulated blood vessels (endothelial cells). In tissue, clusters may also be generated by local T cell proliferation (Ulrichs et al., 2004), which is not included in our model.

The total number of simulated T cells may be greater than it should be due to excessive influx or insufficient T cell death rates. Excessive T cell numbers or densities in the simulations may explain why there is little delay between the initial arrival of T cells and the decline in the *Mtb* population shown in Fig. 3; experiments in mice show a later peak in the bacterial load. There are no estimates of the numbers of different cell types in early lesions for comparison to the simulated lesion cell composition. In patients with latent infection, T cell:macrophage ratios in 5 cm^3 of lung tissue containing mature lesions were approximately 1:3 or 1:2 (Ulrichs et al., 2005). In our simulated 1 mm^3 lesion, this ratio is approximately 3:5.

The ability to make visual comparisons between simulated and actual lesion appearances is a valuable addition to the standard comparisons of population and concentration time courses. Since macrophage activation and T cell cytokine production depend on contact between macrophages and T cells, the spatial relationships between cells are important. A better understanding of the spatial structure within these lesions is needed. It will require both more experimental work at the level of individual lesions and further refinements to spatial models such as ours.

5.3. Timing of T cell influx

In the simulations discussed thus far, T cell influx began 2 weeks after infection, as observed in mice (Chackerian et al., 2002). The time required for expansion of an antigen-specific population of T cells is thought to be less than 1 week (Janeway et al., 1999). However, antigen must reach the lymphoid organs in large enough quantities before this expansion can begin. It is thought that slow bacterial dissemination in tuberculosis infection is responsible for the delayed appearance of *Mtb*-specific T cells (Chackerian et al., 2002). The slow progression observed early in our simulations, due both to slow bacterial growth and slow recruitment of immune system cells, supports the notion that transport of antigen to lymphoid organs would also be slow.

The goal of tuberculosis vaccination is to increase the population of *Mtb*-specific T cells available early in infection in the hopes of preventing disease. However, experiments in mice show that although vaccination reduces the bacterial load, it does not clear the infection (North and Jung, 2004). Simulations in which T cell influx begins 1 week after infection reproduce these experimental models. Figure 6 shows simulated *Mtb* growth curves for T cell delays of 1 and 2 weeks; runs with no T cells are shown for comparison. Earlier T cell arrival allows earlier inhibition of *Mtb* growth and a significant reduction in the bacterial load. However, there is still significant growth within unactivated macrophages in both sets of simulations. Only 2 of 30 simulations with a 1-week delay in T cell influx cleared their pathogens. These results suggest that factors other than the availability of T cells limit the immune system's ability to control the pathogen.

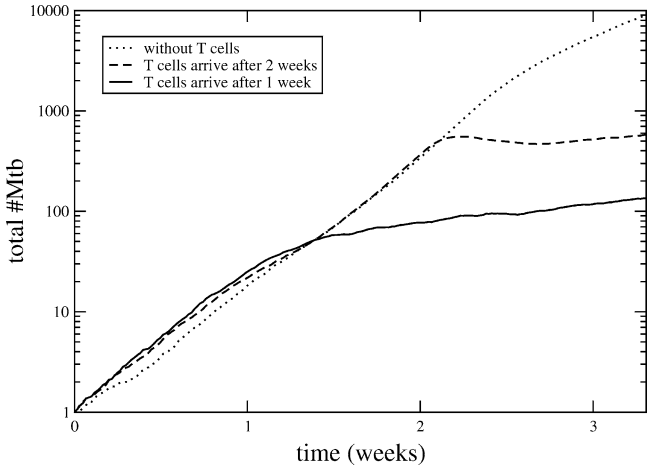

Fig. 6 Effect of earlier T cell influx on simulated *Mtb* growth. $q_{\max} = 2$ per day; other parameter values are same as shown in Table 1.

5.4. IFN-γ receptor deficiency

A genetic susceptibility to mycobacterial infection has been linked to near absence of the primary receptor for IFN-γ, IFN-γR1 (Newport et al., 1996). Experiments with IFN-γR1-deficient mice show that loss of this receptor impairs the ability to control *Mtb* growth (MacMicking et al., 2003). This deficiency is represented in our model by raising the value of m_{IFN} to 2 pg/ml, making macrophages much less sensitive to IFN-γ. This affects both macrophage activation and IFN-γ inhibition of IL-10 production.

The average *Mtb* growth in the IFN-γ receptor deficiency simulations is compared to the earlier simulations in Fig. 7. Although bacterial load is increased compared to the simulation of a normal response, there is still more control of the pathogen than seen in murine experiments (MacMicking et al., 2003). This could be an artifact of the model, or it could represent an actual difference between human and mouse parameter values.

However, the difference in bacterial load between the models of normal response and IFN-γ receptor deficiency is significant. Figure 8 compares the distributions of the two sets of simulation results at day 23. Although there is some overlap, the IFN-γ receptor deficiency model has many simulations for which *Mtb* loads are much higher. The means of these two distributions are significantly different (two-sample *t*-test, $P = 0.005$). Assuming that disease is associated with *Mtb* burdens above a threshold, our results agree with observations that the chances of developing active disease are increased in the IFN-γ receptor deficiency model.

5.5. IL-10 knockout

IL-10, in both in vitro experimental cellular models and in our model (Fig. 1), inhibits inflammation and macrophage activation, with the logical expectation that

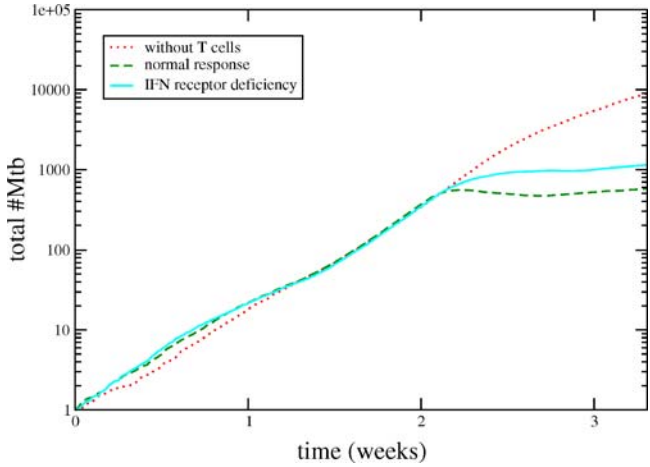

Fig. 7 Average simulated *Mtb* growth with IFN-γ receptor deficiency (*solid line*); results from Fig. 3 included for comparison (*dotted* and *dashed lines*). For *solid line*, $m_{\mathrm{IFN}} = 2$ pg/ml; other parameter values are same as shown in Table 1.

the inhibition of IL-10 would result in increased bacterial killing. When we simulated the absence of IL-10, however, bacterial replication was paradoxically enhanced initially, followed by a marked increase in bacterial killing at 2 weeks when specific T cells were recruited (Fig. 9). These results likely derived from multiple inputs such as longer activation periods and more persistent TNF (chemokine) secretion, and each hypothesis can be tested alone and in combination.

Two animal model studies utilizing IL-10 knockout mice arrived at different endpoints. One study showed an early transient reduction in bacterial loads (Roach, 2001), while the other showed no change in *Mtb* loads in spite of increased IFN-γ production (Jung, 2003). Neither study showed an increase in initial bacterial growth or inflammation. Many possible explanations for the differences

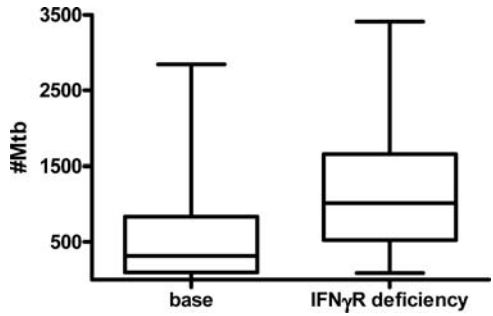

Fig. 8 Effect of IFN-γ receptor deficiency. Distributions of *Mtb* numbers after 23 days for base parameter set and IFN-γ receptor deficiency. The box-and-whisker plot shows median (*line through the box*), first and third quartiles (*ends of the box*), and minimum and maximum values (*lines at the ends of the 'whiskers'*) for each set of simulations.

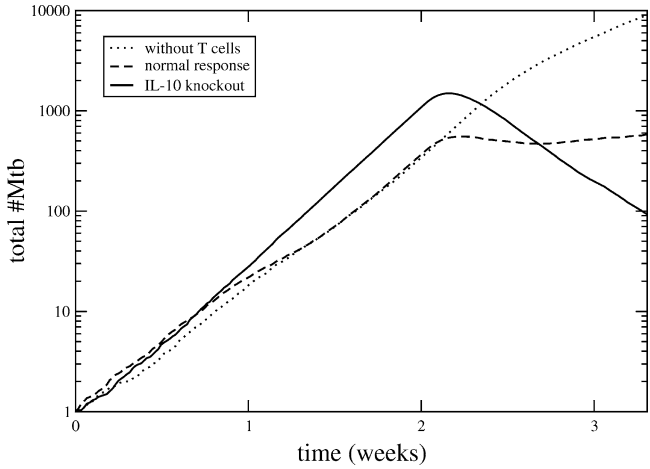

Fig. 9 Average simulated *Mtb* growth with IL-10 knockout (*solid line*); results from Fig. 3 included for comparison (*dotted* and *dashed lines*). For *solid line*, $p_{\mathrm{MIL10}} = p_{\mathrm{TIL10}} = 0$; other parameter values are same as shown in Table 1.

between in silico and in vivo models may pertain. Our model ignored IL-10 inhibition of CD4+ T cell proliferation and cytokine secretion. It also did not distinguish between T cell subsets, and regulatory T cells secreting IL-10 may exhibit different dynamics than that modeled here. The phenotype of IL-10 knockout mice suggests that IL-10 is a key regulator of the balance between pathology and protection, and the current lack of understanding of the complexity of regulatory inputs suggests that it will be difficult to capture this delicate balance faithfully.

5.6. Increased TNF production

Genetic variation in TNF genes is associated with increased levels of TNF and may be associated with increased susceptibility to a number of diseases including some in which pathogens infect macrophages (Hill, 1998). The cause of increased susceptibility and/or pathology in these diseases is not understood. There are no documented associations between increased TNF levels and tuberculosis outcome, but neutralization of TNF secretion by monoclonal anti-TNF antibodies increases susceptibility to clinical tuberculosis (Dinarello, 2005). TNF appears to be an important cytokine in tuberculosis, and variation in TNF production could conceivably be important. We simulated increased TNF production by increasing the model secretion rates p_{MTNF} and p_{TTNF} fivefold.

Figure 10 shows that this change does not significantly affect the *Mtb* growth curve. Increased TNF concentrations lead to increased cell recruitment, more infected cells and small increases in the other cytokines; the increases appear to counteract each other and produce little net change to the bacterial dynamics.

Figure 11 also shows that distributions of bacterial loads are similar ($P > 0.5$), but that lesion sizes are significantly larger ($P = 2.5 \times 10^{-7}$) with increased TNF production. Increased lesion size may be a correlate of increased pathology. On

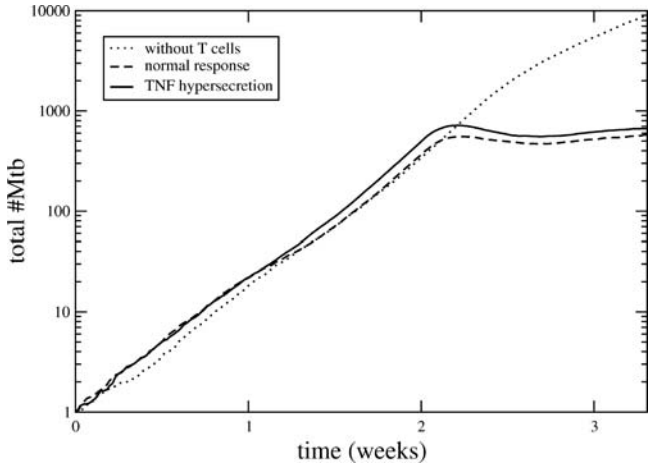

Fig. 10 Average simulated *Mtb* growth with increased TNF secretion (*solid line*); results from Fig. 3 included for comparison (*dotted* and *dashed lines*). For *solid line*, $p_{\mathrm{MTNF}} = 3000$, $p_{\mathrm{TTNF}} = 10{,}000$; other parameter values are same as shown in Table 1.

the other hand, Chackerian et al. (2002) observed that mice that are able to survive *Mtb* infection longer had faster initial lesion growth than more susceptible mice. As in the simulations, bacterial load for the first few weeks was the same in both strains. Chackerian et al. (2002) hypothesized that faster initial growth enhanced development of the T cell response, with beneficial effects later in the infection. This is an example of ways in which individual aspects of the immune response can be either detrimental or beneficial, or perhaps both.

6. Discussion

A key distinction of our model is the focus on early infection dynamics. The typical approach is to characterize the steady-state behavior of the system over weeks to months. We believe that early events are crucial in shaping the eventual outcome

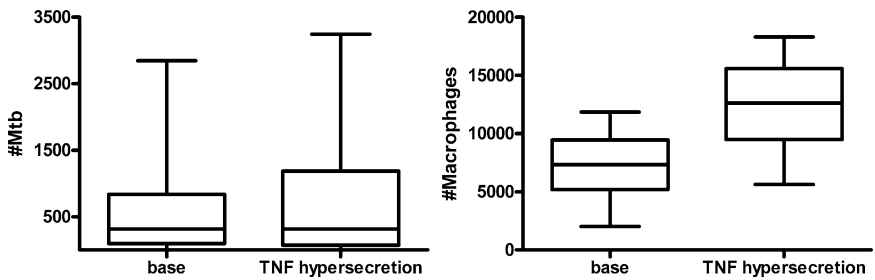

Fig. 11 Effect of increased TNF production. Distributions of *Mtb* load (*left*) and total number of macrophages (*right*) after 23 days for base parameter set and TNF hypersecretion.

of the response. As we observed in Section 5.1, there can be considerable variation in the dynamics over the first few weeks. The fact that there is similar variation in infection outcome in humans and mice illustrates the importance of explicitly representing the heterogeneity that occurs in real cell populations and the effects of stochastic processes. Similarly, Section 5.2 illustrated that the spatial structure of the developing lesion may also be significant. Successfully capturing the spatial interactions between cells may be as important as including greater molecular detail. The biological rationale for modeling spatial interactions is the autocrine/paracrine nature of cell signaling. Our spatiotemporal model of *Mtb* infection has simplified many molecular, cellular, and structural features of the acute immune response in the lung. Despite these limitations, it has produced simulations mimicking several different outcomes repeatedly observed in in vivo models of tuberculosis. Our goal is to capture what is known about TB infection in an executable model that allows us to explore various hypotheses about what is not known.

Our model predicts unrestricted growth of mycobacteria in the presence of macrophages alone, and restricted replication following the influx of immune T cells. Earlier influx of T cells causes lower average mycobacterial numbers by 3 weeks. These qualitative results are observed in mice in vivo (North and Jung, 2004). Clearance of bacteria is rarely demonstrated in animal models. Although T cells activate macrophages, T cells also increase macrophage recruitment contributing to microbial persistence and spread in the model. In the simulations, increased numbers of T cells tended to clump, compromising the efficiency of macrophage activation. Microbial persistence may involve spatial isolation of macrophages from activated T cells. However, our model does not account for other factors such as inherent deficiencies in macrophage mycobacteriocidal capacities or changes in the microbial transcriptome governing evasion mechanisms and reduced intracellular replication (North and Jung, 2004). These are areas for future work.

Our model captures some interesting cytokine effects in early *Mtb* infection. Reduced signaling due to IFN-γ receptor deficiency results in enhanced mycobacterial growth in both murine and human infections (Newport et al., 1996; MacMicking et al., 2003). Our model qualitatively reproduces these observations; the available literature does not permit quantitative comparisons. TNF may activate macrophages and synergize with interferons in this function. In the model, a five-fold increase in TNF secretion had no net effect on mycobacterial replication in the model but caused significant increases in macrophage influx. TNF regulates chemokine induction essential for cell recruitment, granuloma formation, and clearance of mycobacterial infection (Roach et al., 2002; Botha and Ryffel, 2003; Algood et al., 2004). The model set TNF to represent chemokine activity, and therefore TNF was directly responsible for macrophage recruitment. The lack of effect on mycobacterial numbers was not unexpected, since the primary effect of TNF is to aid containment of *Mtb* later in infection (Mohan et al., 2001). The simulation results highlight the contradictory effects of IL-10, which both inhibits inflammation (reducing macrophage influx) and inhibits macrophage activation. They illustrate a two-phase effect, perhaps first expressing the effect of inhibiting macrophage activation, followed by inhibiting inflammation. A more sophisticated

treatment of the complex regulatory interactions mediated by IL-10 will be a fruitful target for future simulations.

Like any model, ours has limitations imposed by the selection of certain features and exclusion of others, by conflicting data in the literature, and by the incomplete knowledge of molecular complexes and signaling pathways of the immune response. Our model did not incorporate the immense diversity of T cell phenotype and regulatory function, nor did it provide a role for NK cells, features that will be incorporated in future models. Cytokines such as TNF and IL-10 modulate effects on apoptosis of infected cells (Oddo et al., 1998; Rojas et al., 1999; Keane et al., 2000) as well as activation. Moreover, the model does not incorporate a signal threshold for activation; the cumulative probability of activation in response to low levels of IFN over time may be overestimated. In the model, local cytokine concentrations are primarily a function of cell density, limited by packing of cells by chemotaxis and repulsion of adjacent cells counteracting chemotaxis. The model does not incorporate receptor-mediated uptake and removal and other negative feedback mechanisms to modulate local cytokine concentrations, nor does it include the effects of cytokine production by local tissue cells. There are also a number of ways in which more anatomic realism could be incorporated. For example, we include necrosis operationally in that infected macrophages die, but we do not include the resulting tissue changes that affect cytokine diffusion and cell movement. The net result of these simplifications is that diffusion is more rapid and cell movement less hindered than in real tissues. As more quantitative experimental data on these local effects become available, we will be able to extend the model accordingly.

Most recent publications on modeling pulmonary tuberculosis and similar diseases use differential equations to describe the persistence of mycobacteria. A simple differential equation model predicted long-term persistence of organisms if non-replicating dormancy was a feature (Antia et al., 1996). The interaction between pathogen clearance and persistence caused oscillations of mycobacterial numbers, a feature not yet demonstrated in in vivo models. A more sophisticated differential equation model incorporating detailed dynamics of cytokine production and immune cell function focused on long-term persistence of mycobacteria in the lung (Wigginton and Kirschner, 2001). This model also predicted oscillations in bacterial numbers over time, arriving at an equilibrium level of persistence. A more recent model by the same group uses an agent-based approach (Segovia-Juarez et al., 2004). Their model is two-dimensional and restricts cells to a fixed lattice, but they conclude as we do that modeling cells in a spatially explicit manner is most appropriate for representing granuloma formation. The contributions of these models and others to understanding tuberculosis has been recently reviewed (Kirschner and Marino, 2005).

CyCells is a multipurpose simulator designed to incorporate spatial and stochastic effects. Two other multipurpose simulators have been developed specifically for multicellular systems and molecular interactions. The biological toolbox (Vawer and Rashbass, 1997) used a mix of unrestricted cell movement and continuous molecular concentrations similar to that in Dallon (2000). SIMMUNE used a regular lattice to define cell positions and discretization of molecular concentrations (Meier-Schellersheim, 2001). However, these programs are not publicly available.

CyCells in its current form can be used to model a wide variety of multicellular systems, and the source code is available for those who wish to extend or modify the simulator implementation (https://sourceforge.net/projects/cycells/).

In our simulations, we qualitatively replicated several outcomes observed in murine models of tuberculosis altered by increase or decrease or removal of key cytokines or their receptors. These replicated features were unexpected because the model represents a marked simplification of the known immune response components. The reasons for our successful replications are not completely understood, but may in part be due to the robust network of host defense components permitting survival in spite of removal of putatively critical molecular components. Further model development will incorporate greater cellular and molecular detail. Ideally, model development will be facilitated by in vivo experiments designed to provide the quantitative details necessary to ultimately arrive at successful predictive models. We believe that these models will incorporate the stochastic and spatiotemporal determinants exemplified in CyCells.

Acknowledgement

This publication was made possible by NSF (grants ANIR-9986555, CCR-0331580 CCR-0311686, and DBI-0309147), DARPA (grants F30602-02-1-0146), NIH Grant Number RR-1P20RR18754 from the Institutional Development Award (IDeA) Program of the National Center for Research Resources, P20 GM066283 and *NIAID U54 AI057156 subaward 05-082*. Its contents are solely the responsibility of the authors and do not necessarily represent the official views of NSF, DARPA, or NIH.

Appendix

A.1. Uninfected state

In the absence of infection, macrophages are assumed to enter the local tissue from circulation at a fixed rate i. They have a fixed death rate l_{M}, which balances the influx rate to maintain a constant population. Uninfected macrophages do not produce any cytokines.

Although influx and death are described in terms of the population rate, simulated cell arrivals and deaths occur with probability $p = r\Delta t$, where r is the population rate and Δt is the time step. Other stochastic events are modeled similarly.

A.2. Phagocytosis and infection

As explained in Section 3.2.2, each simulated macrophage has an attribute representing its phagocytic ability, with values ranging from 0 to 1. Those macrophages with a phagocytic ability greater than ϕ are able to phagocytose *Mtb* that are close enough. Our value for ϕ comes from in vitro data (Engele et al., 2002).

When an uninfected macrophage phagocytoses a bacterium, it becomes infected. Infected macrophages may continue to phagocytose bacteria. *Mtb* replicate inside infected macrophages at a fixed rate in our model. The possible *Mtb* switch into a nonreplicating state (Shi et al., 2003) is assumed to occur after the time period covered by these simulations. Other factors affecting intracellular dynamics are discussed in Section A.4. Some infected macrophages die due to excessive bacterial load, assumed to occur when the number of intracellular bacteria reaches N. When infected cells die, whether due to excessive bacterial load or not, their *Mtb* are released into the extracellular environment.

There is no provision for extracellular *Mtb* growth or death in this model; the bacterial population changes only through ingestion and release by macrophages and intracellular growth and death. Dannenberg and Rook (1994) claim that extracellular growth is not significant in the early stages of infection. There is also evidence that *Mtb* persist within tissues for years without replicating (Manabe and Bishai, 2000; Wayne and Sohaskey, 2001), indicating negligible extracellular death.

A.3. Inflammation

We assume that the macrophage influx rate increases as a saturating function of the local TNF concentration C_{TNF}:

$$i_{C_{\mathrm{TNF}}} = \frac{i_{\max} C_{\mathrm{TNF}}}{i_{\mathrm{half}} + C_{\mathrm{TNF}}} \tag{A.1}$$

where $i_{\max}$ is the maximum influx rate and i_{half} is the TNF concentration at which the actual rate is half-maximal. (Production of TNF is described in Section A.5.) The saturating form reflects the assumption that there is a physical limit on the number of cells that can migrate at once, due either to availability of the cells in circulation or to limits on their passage through the endothelium and epithelium.

The form of Eq. (1) describes T cell recruitment as well, except there is a delay before T cell influx begins, to represent the time required to mount a T cell response. The model ignores possible depletion of cells in circulation; this effect should not be significant for the short-term responses considered here. T cells have a fixed death rate l_{T}.

Parameters describing cell movement and interaction distances are given in Table 2. The speed and persistence times shown are based on studies of macrophages; for simulation purposes, T cells are assumed to move the same way that macrophages do.

A.4. Macrophage activation

Intracellular bacterial replication occurs with probability $g\Delta t$ and death of intracellular bacteria occurs with probability $q\Delta t$ for each bacillus. In unactivated macrophages, $q = 0$. Macrophages are activated by changing the value of q to $q_{\max}$ (referred to in the diagram (Fig. 1) as turning killing on) with probability $a\Delta t$. Kaufmann (2001) notes that even highly activated macrophages may fail to fully

Table 2 Parameters for cell movement and contact.

Parameter	Meaning	Value	Source
S	Cell speed	2 μm/min	Lauffenburger and Linderman (1993)
P	Cell persistence time	30 min	Lauffenburger and Linderman (1993)
R_{M}	Macrophage radius	5 μm	Estimate
R_{T}	T cell radius	3 μm	Estimate
R_{P}	Pathogen radius	1 μm	Estimate
H	Contact distance	10 μm	Estimate
$L_{\min}$	Minimum chemokine concentration	1 pM	Thomson (1998)

Note. Cells and pathogens are represented as spheres with the specified radii for collision resolution purposes. However, since real cells are not spheres and macrophages can extend pseudopods to sense their surroundings, simulated cells respond to neighbors within 10 μm. For chemotactic movement, the chemokine concentration must be greater than $L_{\min}$. Chemokine sensitivities vary, but the value listed is close to 1 molecule per cell volume and therefore represents a reasonable lower bound below which gradients will not be detectable.

eradicate their intracellular pathogens. In the model, the likelihood of this happening depends on the relative values of g and q. If a cell manages to kill all of its intracellular bacilli, it reverts to the uninfected state.

Macrophage activation requires contact between the infected cell and a T cell, and a nonzero IFN-γ concentration. It is probabilistic, with the chances of activation increasing with increasing concentrations of IFN-γ and TNF. The activation probability is assumed to be of the form:

$$a\Delta t = a_{\max}\frac{C_{\mathrm{IFN}}(1 + a_{\mathrm{TNF}}C_{\mathrm{TNF}})}{C_{\mathrm{IFN}}(1 + a_{\mathrm{TNF}}C_{\mathrm{TNF}}) + m_{\mathrm{IFN}}}\Delta t \tag{A.2}$$

where C_{IFN} and C_{TNF} are the concentrations of IFN-γ and TNF, respectively. $a_{\max}$ is the maximum rate at which cells become activated. The estimate for $a_{\max}$ of 1 per day comes from the observation that it takes roughly 1 day to start production of reactive nitrogen intermediates (RNI) thought to be important in control of *Mtb* (Schroder et al., 2004). m_{IFN} represents the concentration of IFN-γ at which the activation rate is half of its maximum value. a_{TNF} represents the synergistic effect of TNF on macrophage activation. Macrophages in the simulation can be activated by IFN-γ alone or in combination with TNF but not by TNF alone.

The probability $u\Delta t$ that a newly infected cell becomes chronically infected (and therefore unable to produce TNF or kill bacteria) increases with increasing concentrations of IL-10:

$$u = u_{\max}\frac{C_{\mathrm{IL-10}}}{C_{\mathrm{IL-10}} + m_{\mathrm{IL-10}}} \tag{A.3}$$

where $C_{\mathrm{IL-10}}$ is the concentration of IL-10, $u_{\max}$ the maximum transition rate, and $m_{\mathrm{IL-10}}$ the IL-10 concentration at which the rate is half-maximal.

A.5. Cytokine production

Differences in cytokine concentrations in culture reflect differences in the number of cytokine-producing cells and in production rates for each cell. Cytokine production depends on transcriptional regulation within individual cells; Hume (2000) suggests that it is more appropriate to think of this regulation in terms of probabilities of transcription rather than rates.

Accordingly, inducible cytokine production in the simulated cells is modeled by giving them a probability of starting or stopping cytokine secretion at a fixed rate. At this time, there is insufficient published data for modeling continuously varying secretion rates.

A.5.1. Macrophage cytokine secretion

Mtb can induce newly infected macrophages to produce TNF and/or IL-10. There are separate probabilities controlling whether or not each cell starts producing each cytokine. The probability of starting TNF secretion is fixed, given by $v_{\text{on}}\Delta t$. We chose a value for v_{on} that allows the average infected cell to start producing TNF about 1 day after infection. The probability $w\Delta t$ of starting IL-10 secretion depends on IFN-γ:

$$w = w_{\max}\frac{m_{\text{IFN}}}{C_{\text{IFN}} + m_{\text{IFN}}} \tag{A.4}$$

In this case, the maximal rate $w_{\max}$ occurs when there is no IFN-γ; increasing concentrations of IFN-γ decrease the probability that a cell will start secreting IL-10. m_{IFN} represents the IFN-γ concentration at which the rate is half-maximal; the same value was used here as in Eq. (2).

Once secretion is "turned on," a cell continues to secrete at a fixed rate until secretion is turned off. The rates are p_{MTNF} and $p_{\text{MIL-10}}$ for TNF and IL-10, respectively. Macrophage IL-10 production is turned off only if the macrophage becomes uninfected. TNF production is turned off when a cell becomes chronically infected, and it may be turned off earlier with probability $v\Delta t$ that increases with IL-10:

$$v = v_{\text{off}}\frac{C_{\text{IL-10}}}{C_{\text{IL-10}} + m_{\text{IL-10}}} \tag{A.5}$$

Parameters for macrophage cytokine secretion were chosen so that the resulting concentrations were in rough agreement with those observed in culture experiments (Engele et al., 2002).

A.5.2. T Cell cytokine secretion

T cell cytokine production requires contact between the T cell and a newly infected macrophage; chronically infected cells lose their ability to stimulate T cell cytokine production. All T cells are assumed to be capable of producing IFN-γ

and TNF when they enter infected tissue. IL-10 production, however, is delayed as reported in Yssel et al. (1992). "Turning on" T cell IL-10 production is modeled similarly to macrophage IL-10 production, using Eq. (4). Cytokine secretion rates are fixed, as for macrophages; the rates are p_{TTNF}, $p_{\mathrm{TIL-10}}$ and p_{TIFN} for TNF, IL-10 and IFN-γ, respectively. T cell secretion parameters were chosen so that the resulting concentrations were in rough agreement with those observed in in vitro experiments (Barnes et al., 1993; Tsukaguchi et al., 1999).

A.6. Cytokine decay and diffusion

All cytokines are assumed to decay and diffuse at fixed rates. The rates used are the same for all cytokines, which have roughly similar molecular weights. In vivo, cells also remove cytokine molecules from the extracellular environment; cytokine concentrations therefore depend on cell density. However, there is insufficient information on binding and internalization rates of the cytokines used in this model to include this effect. Implications of this limitation are discussed in Section 6.

Changes in molecular concentration due to diffusion are calculated using an explicit method based on concentrations from the previous time step. The change in one time step of the concentration u in a particular grid cell with indices i, j, k is given by:

$$\frac{\Delta u_{i,j,k}}{\Delta t} = D\left[\frac{u_{i+1,j,k} + u_{i-1,j,k} + u_{i,j+1,k} + u_{i,j-1,k} + u_{i,j,k+1} + u_{i,j,k-1} - 6u_{i,j,k}}{(\Delta x)^2}\right] \tag{A.6}$$

where D is the diffusion coefficient and Δx is the width of each (cubical) grid cell. For this method to give reasonable results, the time step must meet the following constraint (Press et al., 1998):

$$\Delta t \leq \frac{(\Delta x)^2}{6D} \tag{A.7}$$

If the global simulation time step is larger than this limit, the diffusion routine takes multiple substeps using a smaller time step that meets the constraint.

Our implementation of molecular diffusion does not take the local cell density into account. This is a common simplification, but one that could affect molecular concentrations and gradients in regions of high cell density.

References

Aderem, A., 2003. Phagocytosis and the inflammatory response. J. Infect. Dis. 187(Suppl 2), S340–S345.

Antia, R., Koella, J.C., et al., 1996. Models of the within-host dynamics of persistent mycobacterial infections. Proc. R. Soc. Lond. B. Biol. Sci. 263(1368), 257–263.
Barnes, P.F., Abrams, J.S., et al., 1993. Patterns of cytokine production by mycobacterium-reactive human T cell clones. Infect. Immun. 61(1), 197–203.
Blusse van Oud Alblas, A., Mattie, H., et al., 1983. A quantitative evaluation of pulmonary macrophage kinetics. Cell Tissue Kinet. 16(3), 211–219.
Bonecini-Almeida, M.G., Chitale, S., et al., 1998. Induction of in vitro human macrophage anti-*Mycobacterium tuberculosis* activity: Requirement for IFN-gamma and primed lymphocytes. J. Immunol. 160(9), 4490–4499.
Brookes, R.H., Pathan, A.A., et al., 2003. CD8+ T cell-mediated suppression of intracellular *Mycobacterium tuberculosis* growth in activated human macrophages. Eur. J. Immunol. 33(12), 3293–3302.
Chackerian, A.A., Alt, J.M., et al., 2002. Dissemination of *Mycobacterium tuberculosis* is influenced by host factors and precedes the initiation of T cell immunity. Infect. Immun. 70(8), 4501–4509.
Corbett, E.L., Watt, C.J., et al., 2003. The growing burden of tuberculosis: global trends and interactions with the HIV epidemic. Arch. Intern. Med. 163(9), 1009–1021.
Dallon, J.C., 2000. Numerical aspects of discrete and continuum hybrid models in cell biology. Appl. Numer. Math. 32(2), 137–159.
Dannenberg, A.M.J., Rook, G.A.W., 1994. Pathogenesis of pulmonary tuberculosis: An interplay of tissue-damaging and macrophage-activating immune responses—dual mechanisms that control bacilary multplication. In: Bloom, B.R. (Ed.), Tuberculosis: Pathogenesis, Protection, and Control. ASM Press, Washington, DC.
Davis, J.M., Clay, H., et al., 2002. Real-time visualization of mycobacterium–macrophage interactions leading to initiation of granuloma formation in zebrafish embryos. Immunity 17(6), 693–702.
Dinarello, C.A., 2005. Differences between anti-tumor necrosis factor-alpha monoclonal antibodies and soluble TNF receptors in host defense impairment. J. Rheumatol. Suppl. 74, 40–47.
Ding, A.H., Nathan, C.F., et al., 1988. Release of reactive nitrogen intermediates and reactive oxygen intermediates from mouse peritoneal macrophages. Comparison of activating cytokines and evidence for independent production. J. Immunol. 141(7), 2407–2412.
Engele, M., Stossel, E., et al., 2002. Induction of TNF in human alveolar macrophages as a potential evasion mechanism of virulent *Mycobacterium tuberculosis*. J. Immunol. 168(3), 1328–1337.
Fishman, M.A., Perelson, A.S., 1999. Th1/Th2 differentiation and cross regulation. Bull. Math. Biol. 61, 403–436.
Flesch, I.E., Kaufmann, S.H., 1990. Activation of tuberculostatic macrophage functions by gamma interferon, interleukin-4, and tumor necrosis factor. Infect. Immun. 58(8), 2675–2677.
Fulton, S.A., Cross, J.V., et al., 1998. Regulation of interleukin-12 by interleukin-10, transforming growth factor-beta, tumor necrosis factor-alpha, and interferon-gamma in human monocytes infected with *Mycobacterium tuberculosis* H37Ra. J. Infect. Dis. 178(4), 1105–1114.
Hill, A.V., 1998. The immunogenetics of human infectious diseases. Annu. Rev. Immunol. 16, 593–617.
Hogan, L.H., Macvilay, K., et al., 2001. *Mycobacterium* bovis strain bacillus Calmette-Guerin-induced liver granulomas contain a diverse TCR repertoire, but a monoclonal T cell population is sufficient for protective granuloma formation. J. Immunol. 166(10), 6367–6375.
Hume, D.A., 2000. Probability in transcriptional regulation and its implications for leukocyte differentiation and inducible gene expression. Blood 96(7), 2323–2328.
Janeway, C.A., Travers, P., et al., 1999. Immunobiology: The Immune System in Health and Disease, Current Biology Publications, New York.
Jenkins, M.K., Khoruts, A., et al., 2001. In vivo activation of antigen-specific CD4 T cells. Annu. Rev. Immunol. 19, 23–45.
Kaufmann, S.H.E., 1999. Immunity to intracellular bacteria. In: Paul, W.E. (Ed.), Fundamental Immunology. Lippincott-Raven Publishers, Philadelphia.
Kaufmann, S.H.E., 2001. How can immunology contribute to the control of tuberculosis? Nat. Rev. Immunol. 1(1), 20–30.
Keane, J., Remold, H.G., et al., 2000. Virulent *Mycobacterium tuberculosis* strains evade apoptosis of infected alveolar macrophages. J. Immunol. 164(4), 2016–2020.

Kirschner, D., Marino, S., 2005. *Mycobacterium tuberculosis* as viewed through a computer. Trends Microbiol. 13(5), 206–211.
Lauffenburger, D.A., Linderman, J.J., 1993. Receptors: Models for Binding, Trafficking, and Signaling. Oxford University Press, New York.
Ma, J., Chen, T., et al., 2003. Regulation of macrophage activation. Cell Mol. Life Sci. 60(11), 2334–2346.
MacMicking, J.D., Taylor, G.A., et al., 2003. Immune control of tuberculosis by IFN-gamma-inducible LRG-47. Science 302(5645), 654–659.
Manabe, Y.C., Bishai, W.R., 2000. Latent *Mycobacterium tuberculosis* – persistence, patience, and winning by waiting. Nat. Med. 6(12), 1327–1329.
Meier-Schellersheim, M., 2001. The Immune System as a Complex System: Description and Simulation of the Interactions of its Constitutents. Ph.D. Thesis, University of Hamburg, Hamburg
Mohan, V.P., Scanga, C.A., et al., 2001. Effects of tumor necrosis factor alpha on host immune response in chronic persistent tuberculosis: Possible role for limiting pathology. Infect. Immun. 69(3), 1847–1855.
Moore, K.W., de Waal Malefyt, R., et al., 2001. Interleukin-10 and the interleukin-10 receptor. Annu. Rev. Immunol. 19, 683–765.
Newport, M.J., Huxley, C.M., et al., 1996. A mutation in the interferon-gamma-receptor gene and susceptibility to mycobacterial infection. N. Engl. J. Med. 335(26), 1941–1949.
North, R.J., Jung, Y.J., 2004. Immunity to tuberculosis. Annu. Rev. Immunol. 22, 599–623.
Oddo, M., Renno, T., et al., 1998. Fas ligand-induced apoptosis of infected human macrophages reduces the viability of intracellular *Mycobacterium tuberculosis*. J. Immunol. 160(11), 5448–5454.
Press, W.H., Teukolsky, S.A., et al., 1998. Numerical Recipes in C: The Art of Scientific Computing. Cambridge University Press, Cambridge.
Reinhardt, R.L., Khoruts, A., et al., 2001. Visualizing the generation of memory CD4 T cells in the whole body. Nature 410(6824), 101–105.
Rhoades, E.R., Frank, A.A., et al., 1997. Progression of chronic pulmonary tuberculosis in mice aerogenically infected with virulent *Mycobacterium tuberculosis*. Tuber Lung Dis. 78(1), 57–66.
Rojas, M., Olivier, M., et al., 1999. TNF-alpha and IL-10 modulate the induction of apoptosis by virulent *Mycobacterium tuberculosis* in murine macrophages. J. Immunol. 162(10), 6122–6131.
Schroder, K., Hertzog, P.J., et al., 2004. Interferon-gamma: an overview of signals, mechanisms and functions. J. Leukoc. Biol. 75(2), 163–189.
Segovia-Juarez, J.L., Ganguli, S., et al., 2004. Identifying control mechanisms of granuloma formation during *M. tuberculosis* infection using an agent-based model. J. Theor. Biol. 231(3), 357–376.
Serbina, N.V., Flynn, J.L., 1999. Early emergence of CD8(+) T cells primed for production of type 1 cytokines in the lungs of *Mycobacterium tuberculosis*-infected mice. Infect. Immun. 67(8), 3980–3988.
Shi, L., Jung, Y.J., et al., 2003. Expression of Th1-mediated immunity in mouse lungs induces a *Mycobacterium tuberculosis* transcription pattern characteristic of nonreplicating persistence. Proc. Natl. Acad. Sci. U.S.A. 100(1), 241–246.
Silver, R.F., Li, Q., et al., 1998. Expression of virulence of *Mycobacterium tuberculosis* within human monocytes: Virulence correlates with intracellular growth and induction of tumor necrosis factor alpha but not with evasion of lymphocyte-dependent monocyte effector functions. Infect. Immun. 66(3), 1190–1199.
Stewart, G.R., Robertson, B.D., et al., 2003. Tuberculosis: A problem with persistence. Nat. Rev. Microbiol. 1(2), 97–105.
Thomson, A.W., 1994. The Cytokine Handbook. Academic Press, London, San Diego.
Thomson, A.W., 1998. The Cytokine Handbook. Academic Press, San Diego.
Tsukaguchi, K., de Lange, B., et al., 1999. Differential regulation of IFN-gamma, TNF-alpha, and IL-10 production by CD4(+) alphabetaTCR+ T cells and vdelta2(+) gammadelta T cells in response to monocytes infected with *Mycobacterium tuberculosis*-H37Ra. Cell Immunol. 194(1), 12–20.
Ulrichs, T., Kosmiadi, G.A., et al., 2005. Differential organization of the local immune response in patients with active cavitary tuberculosis or with nonprogressive tuberculoma. J. Infect. Dis. 192(1), 89–97.

Ulrichs, T., Kosmiadi, G.A., et al., 2004. Human tuberculous granulomas induce peripheral lymphoid follicle-like structures to orchestrate local host defence in the lung. J. Pathol. 204(2), 217–228.

Vawer, A., Rashbass, J., 1997. The biological toolbox: A computer program for simulating basic biological and pathological processes. Comput. Methods Programs Biomed. 52(3), 203–211.

Warrender, C., Forrest, S., et al., 2004. Homeostasis of peripheral immune effectors. Bull. Math. Biol. 66(6), 1493–1514.

Wayne, L.G., Sohaskey, C.D., 2001. Nonreplicating persistence of *Mycobacterium tuberculosis*. Annu. Rev. Microbiol. 55, 139–163.

Wigginton, J.E., Kirschner, D., 2001. A model to predict cell-mediated immune regulatory mechanisms during human infection with *Mycobacterium tuberculosis*. J. Immunol. 166(3), 1951–1967.

Young, M.E., Carroad, P.A., et al., 1980. Estimation of diffusion coefficients of proteins. Biotechnol. Bioeng. 22, 947–955.

Yssel, H., De Waal Malefyt, R., et al., 1992. IL-10 is produced by subsets of human CD4+ T cell clones and peripheral blood T cells. J. Immunol. 149(7), 2378–2384.